16èmes Journées de l'Hydrodynamique
27-29 novembre 2018 - Marseille

INFLUENCE DU TRAITEMENT DE L'INTERFACE EAU/AIR DANS LA PROPAGATION DE VAGUE EN CFD

INFLUENCE OF INTERFACE TREATMENT IN WAVE PROPAGATION IN CFD

Young Jun Kim[1,2], Young-Myung Choi[1], Benjamin Bouscasse[1], Sopheak Seng[2], David Le Touzé[1]

young-jun.kim@ec-nantes.fr ; youngmyung.choi@ec-nantes.fr ; benjamin.bouscasse@ec-nantes.fr ; sopheak.seng@bureauveritas.com ; david.letouze@ec-nantes.fr

[1]Laboratoire de recherche en Hydrodynamique, Énergétique et Environnement Atmosphérique (LHEEA) / Ecole Centrale de Nantes, France
[2]Bureau Veritas, France

Résumé

La génération et propagation de vagues dans un solveur numérique pour fluides visqueux sont des éléments essentiels pour réaliser des simulations précises dans le secteur naval/offshore. Dans cette étude, le cas de propagation de vagues bidimensionnelles non-linéaires est traité en considérant plusieurs formulations, le domaine périodique permettant de se focaliser uniquement sur les effets du solveur. La méthode de type capture d'interface Volume of Fluid (VOF) est toujours utilisée mais deux algorithmes de convection sont testés (VOF compressible et IsoAdvector). Deux variations sont utilisées sur l'équation de la quantité de mouvement, en considérant un fluide avec densité continue à travers l'interface ou deux fluides par la methode Ghost Fluid qui applique une condition de saut à l'interface. Les différentes combinaisons font l'objet d'une étude de convergence.

Summary

The wave generation and propagation in a viscous flow solver are essential elements for accurate naval and offshore simulation. The study presents two-dimensional nonlinear wave propagation in a periodic domain, which allows for investigating only the effect of the solver. Various options are tested for the solver, first about the convection equation of the volume of fluid (VOF) and then about the momentum equation. Two options are available for the convection (compressible vof and isoAdvector) and two possibilities are investigated for momentum solver; first considering a one-fluid conservative formulation with continuous density over the interface and then a two-phase flow formulation using the ghost fluid method (GFM) and jump conditions. All combinations between these possibilities are investigated and convergence properties are established.

I – Introduction

The wave propagation in a viscous flow is one of the important part of naval computational fluid dynamic (CFD) applications. However, in the two-phase finite volume method (FVM) framework, it is still challenging to generate the precise desired wave and to limit the dissipation in order to maintain the wave amplitude for the whole simulation. And when this is achieved, the good energy conservation may lead to instabilities in the flow disturbing the correctness of the solution. Furthermore, when computing the practical order of convergence in space and time in a wave propagation problem, even if the dissipation and stability of the solution is satisfactory, the order of convergence achieved is often less than the expected theoretical values. The main reason for all these difficulties is the necessity of free-surface modeling. As an interface treatment is required to reflect the discontinuous property of the free-surface (or the multiphase interface) in the numerical computation.

This paper aims to simulate two-dimensional wave propagation periodic problem using different interface treatment schemes. The theories on the interface treatment scheme is presented in section II. Section III and IV present respectively the simulation set-up of periodic wave propagation and its analysis. The base viscous solver is open source library package OpenFOAM (Version 5.0). Additional numerical implementations are from the library package 'foamStar' which is the software developed with Bureau Veritas (BV) with collaboration with Ecole Cnetrale de Nantes.

II – Mathematical model

II – 1 Typical two-phase flow model

In this section few mathematical models for incompressible two-phase flow are presented. The typical incompressible two-phase flow model is derived based on conditional averaging of two fluid. Following momentum and continuity equations is:

$$\frac{\partial(\rho\mathbf{u})}{\partial t} + \nabla\bullet(\rho\mathbf{u}\mathbf{u}) - \nabla\bullet(\mu(\nabla\mathbf{u})) - \nabla\mathbf{u}\bullet\nabla\mu = -\nabla p_d - (\mathbf{g}\bullet\mathbf{x})\nabla\rho + \sigma_\kappa\nabla\alpha\,, \tag{1}$$

$$\nabla\bullet\mathbf{u} = 0\,, \tag{2}$$

where, $\mathbf{u}$ is the continuous velocity field; ρ is continuous density field which has spatial variation due to two fluids (ρ_{air} = 1.0 Kg/m^2, ρ_{water} = 1000 Kg/m^2); μ is averaged dynamic viscosity ($\mu_{air} = 1.0 \times 10^{-5}$ Ns/m^2, $\mu_{air} = 1.0 \times 10^{-3}$ Ns/m^2); p_d is dynamic pressure; σ_κ is surface tension coefficient and considered negligible ($\sigma_\kappa = 0$) in this paper. The finite volume (FV) representation of Eq.(1) is:

$$\frac{\partial(V_P\rho\mathbf{u})}{\partial t} + \sum_f(\rho\phi_f\mathbf{u}) - \sum_f(\mu(\nabla\mathbf{u})) - \nabla\mathbf{u}\bullet\nabla\mu V_P = -\nabla p_d V_P - (\mathbf{g}\bullet\mathbf{x})\nabla\rho V_P\,. \tag{3}$$

Where, P refers to owner cell's properties; V_P is the volume of cell P; $\rho\phi_f$ is the mass flux of a faces f constructing the cell P. The coupled equations Eq.(3) and Eq.(2) are solved with PISO algorithm ([6], [9]) and explained detail in [8] and [14]. Note that density ρ and mass flux $\rho\phi_f$ should be calculated before the PISO loop.

The VOF method define the phase indicator function α as a volume fraction of water in a cell. Thus, $\alpha = 1$ at fully submerged cell and $\alpha = 0$ in the air. From mass conservation equation, the VOF convection equation can be derived as:

$$\frac{\partial(\alpha)}{\partial t} + \nabla\bullet(\mathbf{u}\alpha) + \nabla\bullet(\mathbf{u}_r\alpha(1-\alpha)) = 0\,. \tag{4}$$

Where, $\mathbf{u}_r$ is relative velocity normal to the free-surface and the third term of LHS is an artificial compression term ([4, 1]) which compress the VOF field to minimize the smearing.

II – 2 Compressive VOF convection algorithm

The typical VOF convection algorithm which is also on the OpenFoam embedded solver interFoam (incompressible, Newtonian two-phase flow solver) is presented. The Eq.(4) can be transformed into FV representation with spatial discretization and off-centered Crank Nicolson temporal discretization:

$$\begin{aligned}\frac{(V\alpha)^{t+h} - (V\alpha)^t}{h} + C_{CN}\sum_f [F_f + F_{rf}]^{t+h} + (1-C_{CN})\sum_f [F_f + F_{rf}]^t = 0\,,\\ F_f = \phi_f\alpha_f \quad F_{rf} = \phi_{rf}\alpha_f(1-\alpha_f)\,,\end{aligned} \tag{5}$$

The value C_{CN} is a Crank Nicolson coefficient where $C_{CN} = 0.5$ yields classical Crank Nicolson scheme and $C_{CN} = 1$ yields Backward Euler scheme.

To solve the bounded and non-smeared VOF field, Eq.(5) is separated into two equations: 'Predictor step Eq.(6)' and 'Corrector step Eq.(7)'.

$$\frac{(V\alpha)^* - (V\alpha)^t}{h} + C_{CN}\sum_f [F_{f,upwind}]^{t+h} + (1-C_{CN})\sum_f [F_{f,upwind}]^t = 0\,. \tag{6}$$

$$\frac{(V\alpha)^{t+h} - (V\alpha)^*}{h} + C_{CN}\sum_f [\lambda F_{Correct}]^{t+h} + (1-C_{CN})\sum_f [\lambda F_{Correct}]^t = 0\,. \tag{7}$$

$$\begin{aligned}F_{Correct} &= (F_{f,HighOrder} + F_{rf,HighOrder} - F_{f,upwind})\\ F_{Total} &= F_{f,upwind} + \lambda F_{Correct}\,.\end{aligned} \tag{8}$$

Here, α^* is a intermediate VOF field and λ is a limiter evaluated from MULES(Multidimensional Universal Limiter for Explicit Solver, [8]) which limits the total flux and guarantees the boundedness of the VOF field. The continuous density field and the mass flux are evaluated for PISO algorithm.

$$\rho = \alpha\rho_{water} + (1-\alpha)\rho_{air}\,, \qquad (\rho\phi)_f = \rho_{water}F_{Total} + \rho_{air}(\phi_f - F_{Total})\,. \tag{9}$$

II – 3 VOF convection with IsoAdvector method

The algorithm of geometric VOF scheme 'IsoAdvector' method is presented in this subsection. Instead of solving Eq.(5) in algebraic way, Roenby et al.([12]) developed a new VOF convection method which uses the isosurface of a cell. From the mass conservation equation, the following equation is satisfied for each cell i:

$$\alpha_i(t+h) = \alpha_i(t) - \frac{1}{V_i}\sum_{faces=F_j}\int_t^{t+h}\int_{F_j} H(\mathbf{x},\tau)\mathbf{u}(\mathbf{x},\tau)d\mathbf{S}d\tau\,. \tag{10}$$

Here, $H(\mathbf{x},t)$ is a phase indicator function at a point and satisfies:

$$H(\mathbf{x},\tau)=\frac{\rho(\mathbf{x},\tau)-\rho_{air}}{\rho_{water}-\rho_{air}}\,,\qquad \alpha_i=\frac{1}{V_i}\int_{V_i}H(\mathbf{x},\tau)dV\,. \tag{11}$$

The physical meaning of the integration on LHS of Eq.(10) is that the total volume of water moves across the face j of cell i during the time interval $[t,t+h]$. To simplify the integral, constant face velocity during the time interval is assumed (Eq.(13)).

$$\Delta V_{i,j}(t,h)=\int_t^{t+\Delta t}\int_{F_j}H(\mathbf{x},\tau)\mathbf{u}(\mathbf{x},\tau)d\mathbf{S}d\tau\,, \tag{12}$$

$$\Delta V_{i,j}(t,h)\approx\frac{0.5(\phi_j(t)+\phi_j(t+h))}{|\mathbf{S}_j|}\int_t^{t+\Delta t}A_j(\tau)d\tau\,. \tag{13}$$

$$A_j(\tau)=\int_{F_j}H(\mathbf{x},\tau)d\mathbf{S}\,. \tag{14}$$

The $A_j(\tau)$ is equal to the time series of submerged area of each face j of cell i. The main objective of IsoAdvector scheme is to calculate the time integration of $A_j(\tau)$. To calculate the time variation of submerged area, IsoAdvector scheme construct the initial isosurface in cell i. The constructed isosurface moves with constant velocity and evaluate the change of submerged area in mesh level. The detail algorithm on isosurface construction, isosurface advection and bounding procedures are explained in [12, 13, 11].

II − 4 Two-phase flow model with ghost fluid method

Instead of using averaged two-phase momentum equation (Eq.(1)), another two-phase flow model taking into account the discontinuous properties at the interface with Ghost Fluid Method (GFM) is considered ([5], [15]). Two-phase flow is modeled like a single phase flow (Eq.(15)), and the discontinuous dynamic pressure and density at the free-surface are considered inside the gradient and Laplacian evaluation algorithm.

$$\frac{\partial(\mathbf{u})}{\partial t}+\nabla\bullet(\mathbf{uu})-\nabla\bullet(\nu(\nabla\mathbf{u}))-\nabla\mathbf{u}\bullet\nabla\mu=-\frac{1}{\rho}\nabla p_d\,, \tag{15}$$

$$\nabla\bullet\mathbf{u}=0\,, \tag{16}$$

The free-surface jump conditions for dynamic pressure and density are given as Eq.(17) and Eq.(18), where the operator $[-]$ stands for the jump of quantities at the interface.

$$[p]=0\,,\qquad [p_d]=-[\rho](\mathbf{g}\bullet\mathbf{x})\,, \tag{17}$$

$$[\frac{1}{\rho}p_d]=0\,. \tag{18}$$

Further details on derivations and implementations on the GFM can be found at [15] and [16].

III – Set-up

Four different combination of solvers based on the mathematical models presented in previous section are investigated. For convenience, each solver are named 'Type A1 and A2' and 'Type B1 and B2' and selected schemes are tabulated in Table 1.

Table 1: Definition of solvers

Solver	VOF solver	Momentum solver
Type A1	Compressive VOF	Averaged two-phase
Type A2	IsoAdvector	Averaged two-phase
Type B1	Compressive VOF	GFM
Type B2	IsoAdvector	GFM

III – 1 Simulation set-up

To investigate the ability of each solver in naval applications, a nonlinear wave propagating to positive x direction in two-dimensional domain is considered. The initial wave velocities and the free-surface positions are evaluated with stream function wave theory [10]. The wave conditions used in previous study ([2]) are applied again and tabulated in Table 2.

The computational domain is exactly one wave length in x-direction. Figure 1 shows the computational domain, boundary conditions and initial VOF field. The periodic boundary condition is applied to 'Inlet' and 'Outlet' boundaries. For the 'bottom' patch, slip boundary condition is applied. For the 'Air' patch, open air boundary condition is applied. To measure the wave, 100 wave probes are installed uniformly from 'Inlet' to 'Outlet' boundary.

Second order Crank Nicolson temporal discretization scheme is used for all solver (Table 1). Due to the stability reason, solver Type A1 and Type A2 used Crank Nicolson discretization with off-centering parameter $C_{oc} = 0.95$ which yields Crank Nicolson coefficient $C_{CN} = 1/(1 + C_{oc})$. In contrast, other solvers used classical Crank Nicolson scheme ($C_{oc} = 1.0$). The convection term of Compressive VOF equation is discretized with second order accurate vanLeer flux limiter [7]. The convection term in the momentum equation is discretized with second order upwind biased linear scheme, and diffusion terms are discretized with central differencing scheme. Also, all gradient terms are discretized with central difference scheme. To minimize the temporal uncertainty, 8 outer (SIMPLE) and 2 inner (PISO) correctors are used. For all variables the residuals were lower than 10^{-7}.

Table 2: Wave condition

Item	Unit	Value
Depth (D)	[m]	0.6
Period (T)	[s]	0.7018
Height (H)	[m]	0.05753
Wave length (λ)	[m]	0.8082
Wave stiffness (kA)		0.24

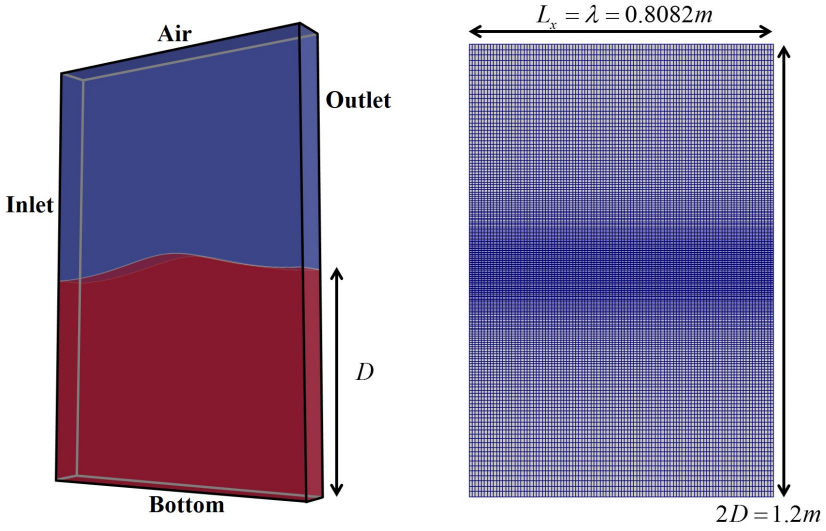

Figure 1: Computational domain and boundary conditions

III – 2 Convergence study set-up

To check the convergence of each solver, a campaign of simulation with five different grids is carried out with similar Courant number. The information on the grid and time step (Δt) are tabulated in Table 3. The refinement factor is $r = 2$ for each level of grid except for the coarsest grid. The uncertainty assessment has performed with the open access tool developed by Eça and Hoekstra ([3]).

Table 3: Mesh for the convergence study (Courant number ≈ 0.17)

Case	$\lambda/\Delta x$	$H/\Delta z$	$T/\Delta t$	$\Delta x/\Delta z$
Grid 1	15	3	50	2.8
Grid 2	25	5	100	2.8
Grid 3	50	10	200	2.8
Grid 4	100	20	400	2.8
Grid 5	200	40	800	2.8

IV – Results and Discussion

This section gives the result of convergence study on four different type of solvers (Table 1). Figure 2 shows the wave profile captured at time $t = 10T, t = 20T, t = 30T$ and $t = 40T$. Figure 3 and Figure 4 present the time averaged first harmonic wave amplitude and phase velocity respect to the refinement level of the mesh (Table 3). The order of convergence P and uncertainty U is evaluated for each type of solver and each time averaged amplitude. No uncertainty assessment has performed for the phase velocity. The summarized order of convergence and uncertainties respect to type of solver and time are arranged on the Table 4.

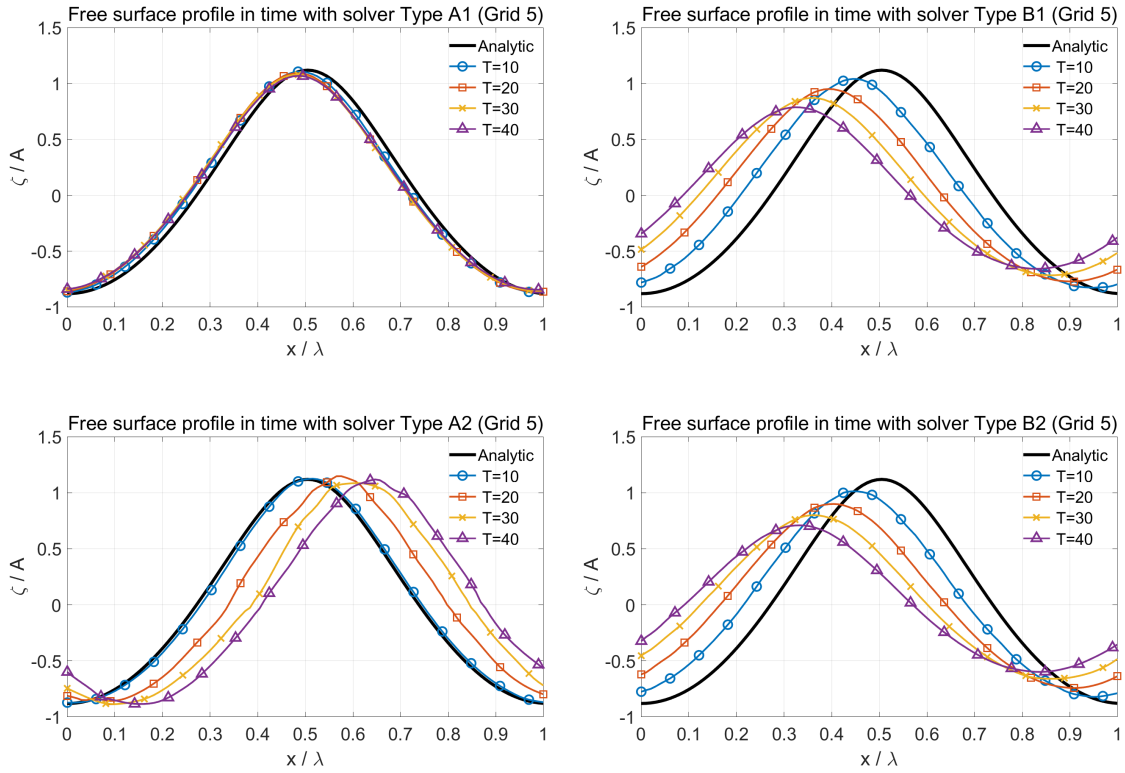

Figure 2: Free surface profile in time with Grid 5

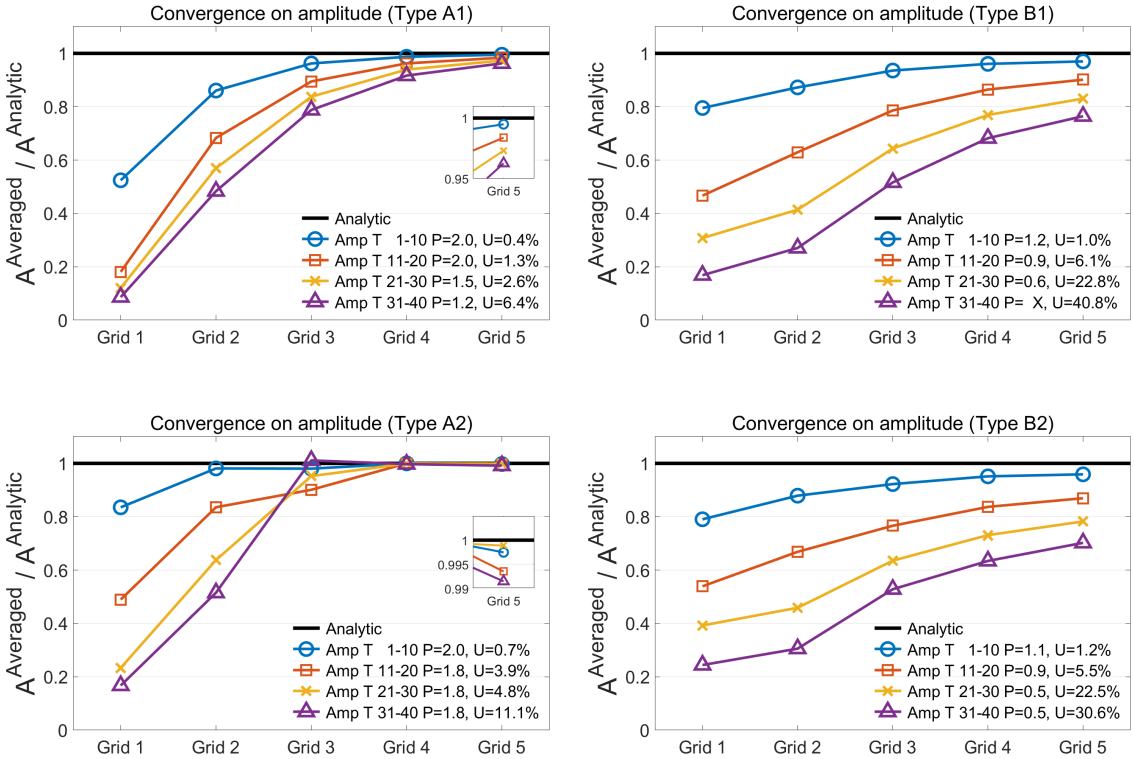

Figure 3: Convergence study on time averaged amplitude

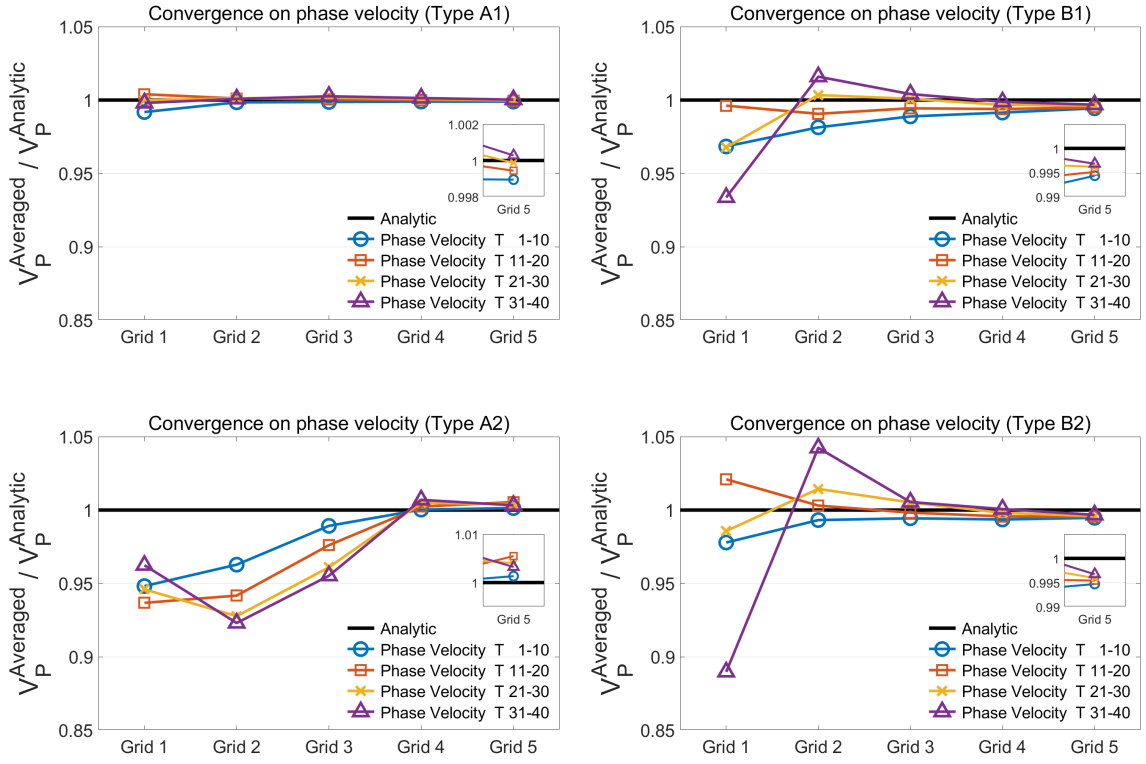

Figure 4: Convergence study on time averaged phase velocity

Table 4: Summary of order of convergence and uncertainties of amplitude

Time	Type A1	Type A2	Type B1	Type B2
Periods 01-10	$P = 2.0$ $U = 0.4\%$	$P = 2.0$ $U = 0.7\%$	$P = 1.2$ $U = 1.0\%$	$P = 1.1$ $U = 1.2\%$
Periods 11-20	$P = 2.0$ $U = 1.3\%$	$P = 1.8$ $U = 3.9\%$	$P = 0.9$ $U = 6.1\%$	$P = 0.9$ $U = 5.5\%$
Periods 21-30	$P = 1.5$ $U = 2.6\%$	$P = 1.8$ $U = 4.8\%$	$P = 0.6$ $U = 22.8\%$	$P = 0.5$ $U = 22.5\%$
Periods 31-40	$P = 1.2$ $U = 6.4\%$	$P = 1.8$ $U = 11.1\%$	$P = X$ $U = 40.8\%$	$P = 0.5$ $U = 30.6\%$

The averaged amplitude from the solvers using averaged two-phase momentum equation (Type A1 and Type A2) show the order of convergence larger than 1 and during the first 10 periods second order convergence is achieved. The 'Type A2' (IsoAdvector) solver gives better conservation of amplitude than 'Type A1' (Compressive VOF) solver. However, the 'Type A2' solver makes wiggles on the interface for the simulation longer than 10 period. Also 'Type A2' solver shows that this solver require at least 100 cell for one wave length to obtain proper phase velocity. But it shows the increase of phase velocity after 10 period.

The solvers using GFM algorithm (Type B1 and Type B2) show lower order of convergence compare to the solver Type A1 and Type A2. The solver Type B1 and Type B2 both showed the convergence for phase velocity but the converged phase velocity is

smaller than the analytic one. The solver Type B1 and Type B2 both show a similar large dissipation of wave amplitude in time and this requires more investigations.

V – ACKNOWLEDGMENT

This work has been performed in the framework of the Chaire Hydrodynamique et Structure Marines CENTRALE NANTES - BUREAU VERITAS.

References

[1] E. Berberović, N. P. van Hinsberg, S. Jakirlić, I. V. Roisman, and C. Tropea. Drop impact onto a liquid layer of finite thickness: Dynamics of the cavity evolution. *Phys. Rev. E*, 79:036306, Mar 2009.

[2] Y. Choi, B. Bouscasse, S. Seng, G. Ducrozet, L. Gentaz, and P. Ferrant. Generation of regular and irregular waves in navier-stokes cfd solvers by matching with the nonlinear potential wave solution at the boundaries. *International Conference on Offshore Mechanics and Arctic Engineering*, Volume 2: CFD and FSI:OMAE2018–78077, 2018.

[3] L. Eça and M. Hoekstra. A procedure for the estimation of the numerical uncertainty of cfd calculations based on grid refinement studies. *Journal of Computational Physics*, 262:104 – 130, 2014.

[4] R. Henric. *Computational Fluid Dynamics of Dispersed Two-Phase Flows At High Phase Fractions*. PhD thesis, Imperial College of Science, Technology and Medicine, 2002.

[5] J. Huang, P. M. Carrica, and F. Stern. Coupled ghost fluid/two-phase level set method for curvilinear body-fitted grids. *International Journal for Numerical Methods in Fluids*, 55(9):867–897.

[6] R. Issa. Solution of the implicitly discretised fluid flow equations by operator-splitting. *Journal of Computational Physics*, 62(1):40 – 65, 1986.

[7] B. V. Leer. Towards the ultimate conservative difference scheme. iv. a new approach to numerical convection. *Journal of Computational Physics*, 23(3):276 – 299, 1977.

[8] S. Márquez Damián. *An extended mixture model for the simultaneous treatment of short and long scale interfaces*. PhD thesis, Universidad Nacional del Litoral, Santa Fe, Argentina, 2013.

[9] S. V. Patankar. *Numerical heat transfer and fluid flow*. Series on Computational Methods in Mechanics and Thermal Science. Hemisphere Publishing Corporation (CRC Press, Taylor & Francis Group), 1980.

[10] M. M. Rienecker and J. D. Fenton. A fourier approximation method for steady water waves. *Journal of Fluid Mechanics*, 104:119–137, 1981.

[11] J. Roenby. *IsoAdvector*. https://github.com/isoadvector.

[12] J. Roenby, H. Bredmose, and H. Jasak. A computational method for sharp interface advection. *Royal Society Open Science*, 3:160405, Nov. 2016.

[13] J. Roenby, H. Bredmose, and H. Jasak. *IsoAdvector: Geometric VOF on general meshes*. Selected papers of the 11th Workshop, 2017.

[14] S. Seng. *Slamming and whipping analysis of ships*. PhD thesis, Technical University of Denmark, 2012.

[15] V. Vukčević. *Numerical modelling of coupling potential and viscous flow for marine applications*. PhD thesis, University of Zagreb, 2016.

[16] V. Vukčević, H. Jasak, and I. Gatin. Implementation of the ghost fluid method for free surface flows in polyhedral finite volume framework. *Computers & Fluids*, 153:1 – 19, 2017.